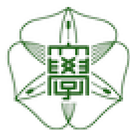
HOKKAIDO UNIVERSITY

Title	Photoelectrochemical Etching Technology for Gallium Nitride Power and RF Devices
Author(s)	Horikiri, Fumimasa; Fukuhara, Noboru; Ohta, Hiroshi; Asai, Naomi; Narita, Yoshinobu; Yoshida, Takehiro; Mishima, Tomoyoshi; Toguchi, Masachika; Miwa, Kazuki; Sato, Taketomo
Citation	IEEE transactions on semiconductor manufacturing, 32(4), 489-495 https://doi.org/10.1109/TSM.2019.2944844
Issue Date	2019-11
Doc URL	http://hdl.handle.net/2115/76692
Rights	© 2019 IEEE. Personal use of this material is permitted. Permission from IEEE must be obtained for all other uses, in any current or future media, including reprinting/republishing this material for advertising or promotional purposes, creating new collective works, for resale or redistribution to servers or lists, or reuse of any copyrighted component of this work in other works.
Type	article (author version)
File Information	IEEE_TSM_Horikiri_91983.pdf

Instructions for use

Hokkaido University Collection of Scholarly and Academic Papers : HUSCAP

Photoelectrochemical Etching Technology for Gallium Nitride Power and RF Devices

Fumimasa Horikiri, Noboru Fukuhara, Hiroshi Ohta, Naomi Asai, Yoshinobu Narita, Takehiro Yoshida, Tomoyoshi Mishima, *Senior Member, IEEE*, Masachika Toguchi, Kazuki Miwa, and Taketomo Sato

***Abstract*— Photoelectrochemical (PEC) etching was used to fabricate deep trench structures in GaN-on-GaN epilayers grown on n-GaN substrates. The width of the side etching was less than 1 μm, with high accuracy. The aspect ratio (depth/width) of a 3.3-μm-wide trench with a PEC etching depth of 24.3 μm was 7.3. These results demonstrate the excellent potential of PEC etching for fabricating deep trenches in vertical GaN devices. Furthermore, we simplified the PEC etching technology to permit its use in a wafer-scale process. We also demonstrated simple contactless PEC etching technologies for the manufacture of power and RF devices. A trench structure was fabricated in a GaN-on-GaN epilayer by simple contactless PEC etching. The role of the cathodic reaction in contactless PEC etching is discussed in relation to the application of a GaN HEMT epilayer on a semi-insulating substrate. Fortunately, the GaN HEMT structure contains an ohmic electrode that can act as a cathode in contactless PEC etching, thereby permitting the recess etching of a GaN HEMT epilayer grown on a semi-insulating SiC substrate. These results indicate that PEC etching technologies are becoming suitable for use in the fabrication of practical GaN power and RF devices.**

***Index Terms*—Gallium Nitride, Etching, Photoelectrochemistry, Trench Fabrication, Recess, Power Devices**

I. Introduction

Gallium nitride (GaN) vertical power devices have recently attracted much attention as energy-saving solutions because of their many advantages in terms of a low specific on-resistance (R_{on}) coupled with a high breakdown voltage (V_B) [1]. Several types of GaN vertical power devices have been reported; these include a trench gate metal oxide conductor field-effect transistor [2,3], a current aperture vertical electron transistor [4,5], a transistor using a fin structure (finFET) [6], and superjunction (SJ) structures [7]. The fabrication of such devices requires the production of trenches and/or apertures. In particular, in the case of SJ structures that are used in Si power devices, to permit unipolar operating limits to be exceeded [8,9], it is necessary to fabricate deep trench structures in an n-type layer with a high depth-to-width aspect ratio that are subsequently backfilled with p-GaN. However, it is difficult to etch deep trenches in GaN. Generally, GaN is etched by inductively coupled plasma reactive-ion etching (ICP-RIE) [10,11]. Unfortunately, however, plasma treatment readily causes damage to GaN, and there is low etching selectivity between the GaN and the etching mask.

Photoelectrochemical (PEC) etching might solve these problems [12–15] as it has excellent etching selectivity against the etching mask and is less likely to cause damage, because it is a plasma-free process. PEC etching has recently been applied to the mesa fabrication of GaN pn-junction diodes (PNDs) with high V_B values [16]. Furthermore, PEC etching produces greater yields of high-V_B devices than does the dry etching of GaN PNDs. Another application of PEC etching is the gate-recess etching for AlGaN/GaN HEMTs [17]. In particular, PEC etching has many advantages from the viewpoint of its self-stopping feature in the gate-recess etching process through modulation of the photoirradiation intensity [12,17]. Here, we report the use of PEC etching in the fabrication of deep trench structures in a GaN-on-GaN epilayer. We also report a simple contactless process for PEC etching that does NOT require any electrical contact with the sample. In addition, we provide examples of the application of simple contactless PEC etching technologies in the fabrication of power and RF devices.

II. Photoelectrochemical Etching Technologies

A. Fundamentals of conventional PEC etching

PEC etching of GaN proceeds by photo-assisted anodic oxidation. GaN is dissolved as Ga^{3+} ions, owing to the presence of holes excited by UV irradiation at the anode of the GaN/electrolyte interface. The resulting Ga^{3+} ions react with hydroxide ions (OH^-) in the electrolyte to form Ga_2O_3. This oxide dissolves in acids or bases. An anodic oxidation process therefore serves as the basis of PEC etching of GaN [12,14,18,19]. The overall etching reaction for GaN, in which

Parts of this study have been reported as F. Horikiri et al., *Proc. CS ManTech*, 2019, Presentation No. 10.3; *Appl. Phys. Express* **11** (2018) pp. 091001-1-4; and *Appl. Phys. Express* **12** (2019) pp. 031003-1-6. This work was supported in part by the Japan Ministry of the Environment as part of the project 'Technical Innovation to Create a Future Ideal Society and Lifestyle'.

F. Horikiri, N. Fukuhara, Y. Narita, and T. Yoshida are with the Engineering Department, SCIOCS Co., Ltd., Hitachi, 319-1418, Japan (e-mail: horikirif@sc.sumitomo-chem.co.jp).

H. Ohta, N. Asai, and T. Mishima are with the Research Center of Ion Beam Technology, Hosei University, Tokyo 184-8584, Japan.

M. Toguchi, K. Miwa, and T. Sato are with the Research Center for Integrated Quantum Electronics, Hokkaido University, Sapporo, 060-0813, Japan.

photogenerated holes (h^+) are consumed, is shown below:

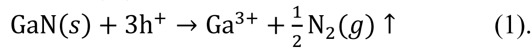

$$\mathrm{GaN}(s) + 3\mathrm{h}^+ \rightarrow \mathrm{Ga}^{3+} + \tfrac{1}{2}\mathrm{N}_2(g)\uparrow \quad (1).$$

In the electrochemical reaction, the total current flowing in the external circuit equals the charge consumed in the reactions at the anode and the cathode. Thus, hydrogen is evolved at the Pt cathode, to which electrons flow from the external circuit, as shown below:

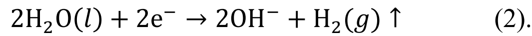

$$2\mathrm{H_2O}(l) + 2\mathrm{e}^- \rightarrow 2\mathrm{OH}^- + \mathrm{H}_2(g)\uparrow \quad (2).$$

In our PEC etching process, the electrolyte was a 0.01 M aqueous solution of NaOH containing 1% Triton X-100 [4-(1,1,3,3-tetramethylbutyl)phenyl-poly(ethylene glycol)]. The latter is a nonionic surfactant that serves as a wetting agent to reduce the surface tension and to assist in the removal of bubbles from the epi surface. A Pt counter electrode was used as the cathode. The anode was a GaN epi surface with a back-side ohmic contact on the substrate. The etching voltage was biased between the GaN epi surface and the Pt counter electrode. The intensity of UV illumination from a Hg–Xe lamp was 9.0 mW/cm^2. A pulsed PEC mode was used in which the UV irradiation and the etching voltage were both applied simultaneously during the PEC step only, and the electrolyte was refilled by using a pump after the PEC step. The next PEC step was started after an interval, because it was necessary to wait until the electrolyte was static. A schematic representation of the PEC etching process is shown in Fig. 1. More details of the procedure can be found elsewhere [14,15].

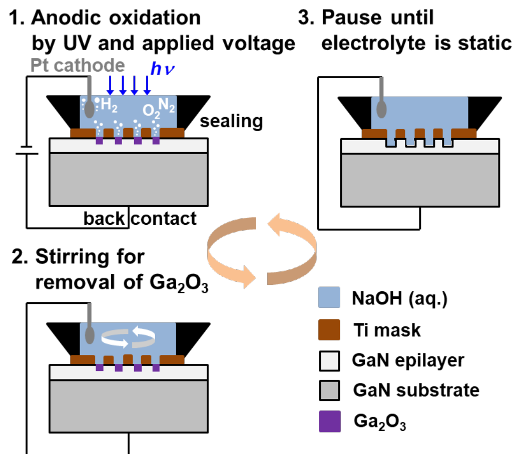

Fig. 1. Schematic representation of the conventional PEC etching of GaN. (Reprinted with permission from [15]; © 2018, Japan Society of Applied Physics.)

B. Simple contactless PEC etching

Conventional PEC etching requires three simultaneous conditions:

(1) UV irradiation at an energy greater than the GaN bandgap,
(2) sealing of the electrolyte between the GaN-surface anode and the cathode, and
(3) electrical contact between the GaN anode and the cathode through an external circuit.

These simultaneous requirements represent a considerable constraint on experimental setups for large-scale wafer-fabrication processes.

There are reports in the literature [19,20] of the use of the sulfate radical ($SO_4^{\bullet-}$) as an oxidizing agent to consume extra UV-photogenerated electrons to provide an electrode-free process. We have previously succeeded in developing a simple electrodeless PEC etching process for wafer fabrication in which the sample was merely dipped into the electrolyte under UV irradiation [20,21].

In contactless PEC etching, an aqueous solution of $K_2S_2O_8$ is generally used as the oxidizing agent. The $S_2O_8^{2-}$ ion absorbs UV irradiation of wavelength <310 nm to form two $SO_4^{\bullet-}$ radicals. The $SO_4^{\bullet-}$ radical is known to be a strong oxidizing agent that has a larger redox potential in the negative direction than that of hydrogen peroxide (H_2O_2). When the $SO_4^{\bullet-}$ radical oxidizes the substrate, it is converted into its reduced form, the sulfate ion (SO_4^{2-}), as follows: $SO_4^{\bullet-} + e^- \rightarrow SO_4^{2-}$. The photo-assisted chemical reaction of GaN in the present redox system can therefore be represented as follows [22]:

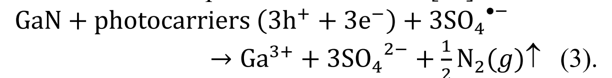

$$\mathrm{GaN} + \text{photocarriers}\ (3\mathrm{h}^+ + 3\mathrm{e}^-) + 3\mathrm{SO_4}^{\bullet-} \rightarrow \mathrm{Ga}^{3+} + 3\mathrm{SO_4}^{2-} + \tfrac{1}{2}\mathrm{N}_2(g)\uparrow \quad (3).$$

Here, descriptions of intermediate products such as Ga_2O_3 are omitted for the sake of simplicity.

A deep-UV flexible-surface light source with a luminous array film (Shikoh Tech LLC) was used as a source of short-wavelength UVC radiation [21]. A 1:1 mixture of 0.01 M KOH (aq.) and 0.05 M $K_2S_2O_8$ (aq.) was used as an electrolyte. The electrolyte depth $d_{electrolyte}$ was set to 5 mm, and the intensity of irradiation at the electrolyte surface was 4 mW·cm^{-2} at 260 nm. Because $K_2S_2O_8$ (aq.) absorbs UV radiation at 260 nm, we designed the experimental layout shown in Fig. 2 so that half of the UVC was consumed in the generation of the sulfate radical ($SO_4^{\bullet-}$) and the remaining half was absorbed at the GaN surface with the formation of photogenerated hole–electron pairs. This layout requires only a single source of UVC.

Unlike the case of conventional PEC etching, the role of the cathode reaction in contactless PEC etching remains unclear [19,20]. In particular, its effect on the etching rate in samples fabricated on semi-insulating substrates, such as sapphire or SiC remains unknown. Here, we investigated the role of cathode in simple contactless PEC etching of GaN for use in fabricating an AlGaN/GaN HEMT RF device on a semi-insulating substrate. The dependence of the cathode ratio per unit area of sample surface on the etching rate is discussed.

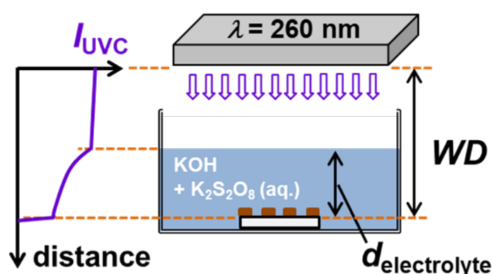

Fig. 2. Schematic representation of the simple contactless PEC etching of GaN. (Reprinted with permission from [21]; © 2019, Japan Society of Applied Physics.)

C. *Epi sample structures*

Epitaxial layers with the structures of Schottky barrier diodes (SBDs) and PNDs were grown by metalorganic vapor-phase epitaxy (MOVPE) on n-GaN substrates. The SBDs consisted of an n-GaN layer with a nominal Si concentration of 1.5×10^{16} cm^{-3} and a thickness of 5.8 μm. The PNDs consisted of a Mg-doped (2×10^{20} cm^{-3} with 20 nm thickness and 5×10^{18} cm^{-3} with 500 nm thickness) layer of GaN on an n^--drift layer of Si-doped (2×10^{16} cm^{-3} with 10 μm thickness) GaN. A 2-μm-thick n^+-interlayer was grown between the n^--drift layer and the n-type GaN substrate. The PNDs were annealed at 850 °C for 30 minutes in N_2 to activate the Mg acceptors before the mask-patterning process. The etching mask was a 50-nm-thick layer of Ti produced by vacuum evaporation with lift off.

In the contactless PEC etching, it was additionally prepared an n-GaN (2 μm)/undoped-GaN (3 μm) epilayer which was grown on a sapphire substrate by MOVPE. The Si donor concentration of the n-GaN layer was nominally 1.2×10^{16} cm^{-3}. A 330-nm-thick SiO_2 mask was prepared by the spin-on-glass method and patterned by using buffered hydrofluoric acid with a photoresist mask. The SiO_2 mask aperture ratio was 49.6% of the surface area. A part of SiO_2 mask was additionally etched to produce apertures, and Ti was deposited as cathode pads covering 0.56, 1.1, 2.2, 4.4, or 7.8% of the surface area, respectively. Ti-masked samples were also prepared with a cathode-pad ratio of 50.4%. Each sample for etching was cut to a size of 6×6 mm^2. Details are discussed below along with the experimental results (see Fig. 8).

III. Results and Discussion

A. *GaN Trench fabrications for power devices*

First, we confirmed that the Ti mask adhered to the p-type layer of the PNDs during the PEC etching process by using a circular-dot mask pattern, because this interface is probably the weakest point in side etching owing to the existence of holes. To demonstrate the potential of PEC etching in deep-trench fabrication, PEC etching was conducted to an etching depth of more than 20 μm with the etching time of about 13 hours. Figure 3(a) shows scanning electron microscopy (SEM) images of typical cylindrical PND patterns produced by conventional PEC etching. The size of the etched region remained almost the same as that of the etching mask, even after etching to a depth of over 20 μm. The width of the side etching was less than 1 μm, with high accuracy. Although it was difficult to evaluate the residual thickness of the Ti exactly, the estimated etching selectivity against the Ti etching mask was >400 (~20 μm/50 nm). The etching rate was approximately 25 nm/min, which is comparable to that of conventional dry etching. The p-GaN etching rate was approximately 1/3 of n-GaN layer. Although PEC etching of p-GaN is difficult, the accumulation of photo-generated holes from PN-junction to p-GaN layer might be pushed the anodic oxidation.

Figure 3(b) shows SEM images of a conventional PEC-etched cavity-shaped SBD pattern with an etching depth of approximately 7.7 μm, as an example of a negative–positive reversal pattern. The diameters of the circular cavities were designed to be 1, 5, 10, and 20 μm. The side walls are almost vertical, and there were small bumps on the bottoms of the circular cavities of 20 μm diameter. Dark spots were observed in SEM-cathodoluminescence images of the centers of the bumps; therefore, the origins of the bumps were dislocations that caused short lifetimes. These PEC-etched cylinder and cavity shapes were independent of the crystallographic orientation; this also indicates that the width of side etching is determined by the hole lifetime.

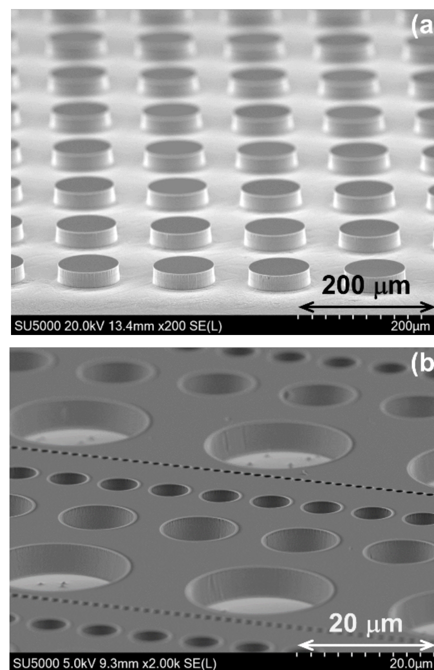

Fig. 3. SEM images of conventional PEC-etched cylinder-shaped (a) and cavity-shaped GaN pattern (b). (Reprinted with permission from [15]; © 2018, Japan Society of Applied Physics.)

GaN vertical trenches were fabricated by using a Ti line mask with a width of 1.4, 2.8, or 5.6 μm on an SBD epi wafer. Figure 4 shows typical cross-sectional SEM images of the trenches produced by conventional PEC etching, cleaved along the *a*-face. Remarkably, each trench had almost the same PEC etching depth of around 7.7 μm; in other words, the depth-etching rate in each pulsed step was controlled by changing the current density.

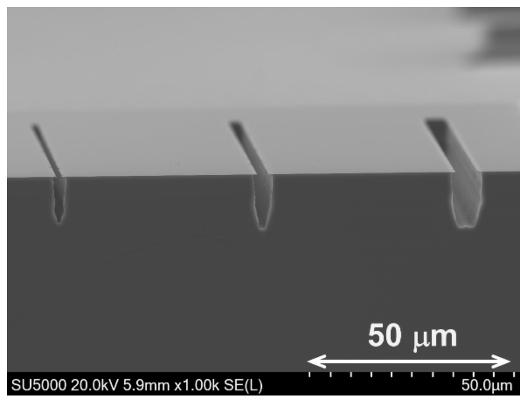

Fig. 4. Typical cross-sectional SEM images of PEC-etched GaN trench patterns, cleaved along the *a*-face.

Figure 5 shows the relationship between the PEC etching depth W_r and the trench aspect ratio. Unfortunately, there are only a few previous reports on the fabrication of GaN vertical trenches. Previously reported GaN trench depths were approximately 1–3 μm with aspect ratios of 1–3. We therefore used SiC trench structures fabricated by ICP-RIE as our reference structures [23–25]. In Fig. 5, the solid, dashed, and dotted lines correspond to estimates of the aspect ratio of PEC etching based on $W_r = (W_{mask} + 2W_{side\text{-}etching})$, where W_{mask} is the width of the Ti etching mask and $W_{side\text{-}etching}$ is the amount of side etching. The width of the side etching was assumed to be 0.7 μm from Fig. 4. The aspect ratio proportionally increased with the etching depth. It indicates that the lateral etching stays almost constant, because the amount of the side etching is determined by the holes lifetime.

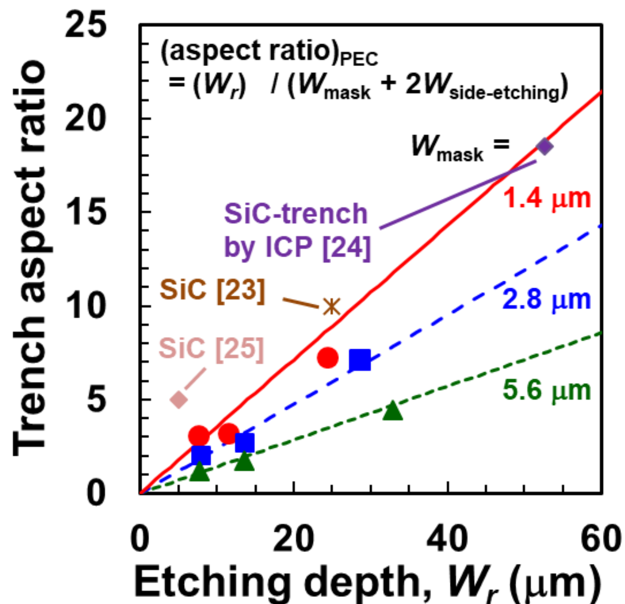

Fig. 5. Relationship between the PEC etching depth W_r and the trench aspect ratio. The solid, dashed, and dotted lines correspond to estimates based on the hypothesis that the aspect ratio of PEC obeys the equation $W_r = (W_{mask} + 2W_{side\text{-}etching})$. The mask aperture width, W_{mask}, was 1.4, 2.8, 5.6 μm. The width of the side etching was assumed to be 0.7 μm from Fig. 4. The filled symbols are experimental results. (Reprinted with permission from [15]; © 2018, Japan Society of Applied Physics.)

With short-width aperture masks, the PEC etching rate showed a decrease at an etching depth of about 30 μm, because the UV radiation appeared to have difficulty in reaching the bottom of these deep trenches. This indicates that a coherent UV light source might be preferable for deep PEC etching. As a matter of fact, the results from Fig. 5 indicate that PEC etching has excellent potential for deep-trench etching. The aspect ratio (depth/width) of the trenches was more than 7 at an etching depth in excess of 20 μm. This aspect ratio and the etching depth are comparable to the best results for SiC trenches fabricated by ICP-RIE.

B. Contactless PEC etching and TMAH posttreatment

Figure 6 shows a plot of the etching depth against the etching time in simple contactless PEC etching of GaN-on-GaN epilayers grown on n-GaN substrates [21]. The etching rate with a Ti mask was approximately 5 nm min^{-1}, which is five times higher than that with a SiO_2 mask. Van Dorp reported that the Pt acts a cathode in contactless PEC etching, whereby hydrogen formation occurs together with electron consumption [20]; the difference in the etching rate between a Ti and a SiO_2 mask indicates the same phenomenon occurs on the surface of the Ti mask. In addition, in GaN-on-GaN chip samples, the side wall fabricated by the chipping process of dicing might act as a cathode, where the UV irradiation was limited. Thus, the photo-generated extra electrons might be consumed by SO_4^- radicals at n-GaN substrate side wall [22], because of existence of holes is limited. We also confirmed that etching did not occur when the side wall and the back-side were covered by photoresist. That is, the cathode should be appropriately designed for a GaN epi layer grown on semi-insulating substrate in contactless PEC etching. The details are discussed in the next section.

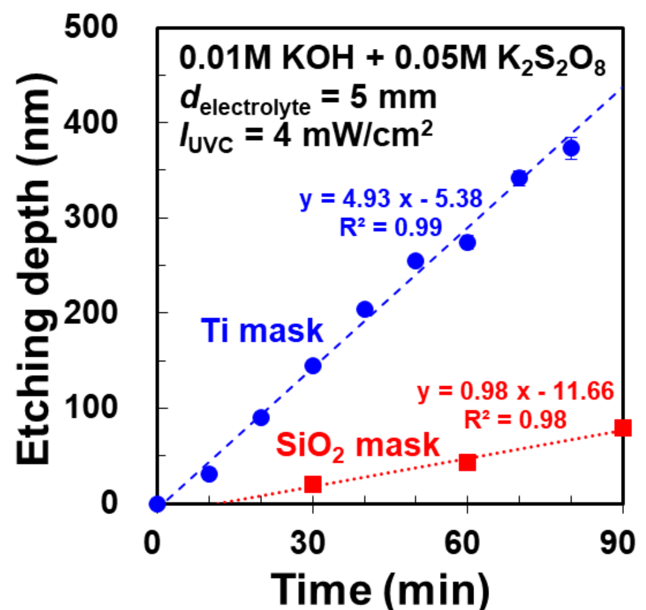

Fig. 6. Results of contactless PEC etching with a catalytic Ti mask, compared with those obtained by using an SiO_2 mask. (Reprinted with permission from [21]; © 2019, Japan Society of Applied Physics.)

Figure 7 shows typical SEM images of surfaces etched by conventional and contactless PEC processes. Treatment by tetramethylammonium hydroxide (TMAH) is a well-known technique for producing vertical side walls in GaN. A 25 wt% aqueous solution of TMAH was used for posttreatment at 85 °C for 30 or 70 minutes. Figures 7(b) and 7(d) show that the TMAH posttreatment was effective in forming vertical side walls in both conventional and contactless PEC etching.

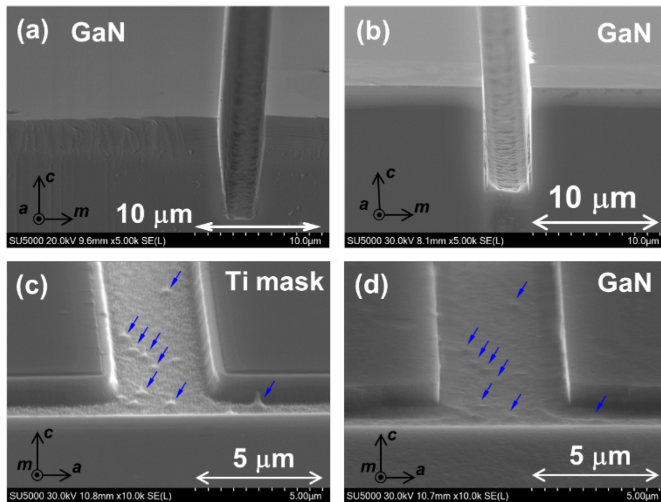

Fig. 7. Typical SEM images of surfaces etched by the conventional and contactless PEC processes. (a) and (b) Surface from conventional PEC etching before (a) and after (b) TMAH posttreatment for 30 minutes. (c) and (d) Surface by from contactless PEC etching before (c) and after (d) TMAH posttreatment for 70 minutes. (Reprinted with permission from [21]; © 2019, Japan Society of Applied Physics.)

C. Cathode design for contactless PEC etching for RF devices

Figure 8 shows typical optical micrographs of n-GaN-on-sapphire samples with various cathode-pad ratio in the range 0.0056–0.504. These six TEST mask patterns have same mask aperture ratio with 0.496 in each 6 × 6 mm^2 sample. The cathode-pad ratios was varied in the range 0.0056–0.504.

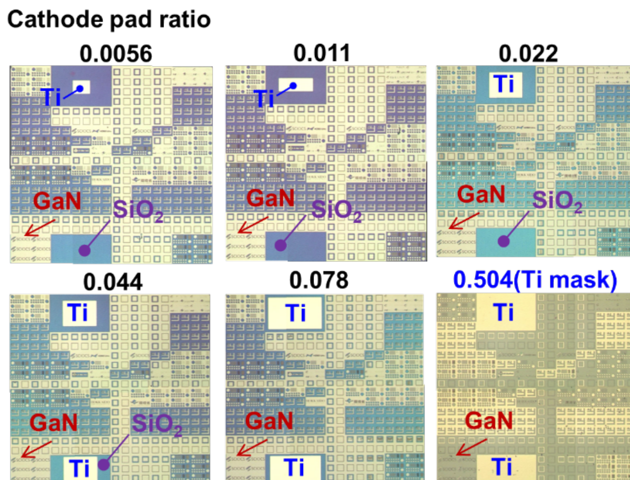

Fig. 8. Typical optical micrographs of n-GaN-on-sapphire samples with various cathode-pad ratios in the range 0.0056–0.504. The each sample size was 6 × 6 mm^2 and the aperture ratio was 0.496.

Figure 9 shows the average rate of contactless PEC etching during 0–120 minutes of n-GaN-on-sapphire samples with various cathode-pad ratios. The etching rate was negligibly small in the sample without a Ti cathode pad, and increased with increasing cathode-pad ratio. These results indicate that an appropriate cathode design is required for samples on semi-insulating substrates. This is important information in relation to the application of simple contactless PEC etching in the fabrication of RF GaN HEMT devices.

Fortunately, HEMT devices have large areas of ohmic electrodes (source and drain) that are potentially useful as cathode pads for contactless PEC etching process. In addition, the isolation and/or gate-recess area is usually outside the ohmic electrode. Thus, the current path between the anode and the cathode pad is maintained during the etching process.

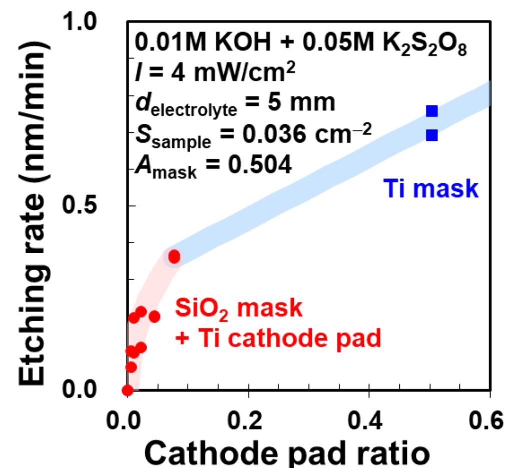

Fig. 9. Average rate of contactless PEC etching during 0–120 min for n-GaN-on-sapphire samples with various cathode-pad ratios.

Figure 10 shows microscopic images of a typical contactless PEC-etched HEMT epi wafer consisting of a GaN/$Al_{0.22}GaN$ (5/24 nm) barrier layer with a 0.75 μm GaN buffer layer on a semi-insulating SiC substrate. In this experiment, we used 0.025 M $K_2S_2O_8$ (aq.) as a simple electrolyte solution. Interestingly, Ti-masked samples has non-etched region around 2–5 μm from the Ti-mask edge. On the other hand, the interface was fine in the sample with a SiO_2 mask and a Ti cathode pad. In electrochemical terms, the anode reaction where GaN etching occurs should be spatially separated from the cathode. Thus, the use of semi-insulating SiO_2 as an etching mask is preferred in contactless PEC etching of an AlGaN/GaN HEMT epi wafer. Moreover, Fig. 10(b) shows that part of the SiO_2 mask was peeled off by side etching, because photogenerated holes were also present below the SiO_2 mask. Therefore, the use of a UV-nontransparent photoresist mask is preferable. We have also found that a positive-type photoresist can be used as the etching mask for a H_3PO_4-based solution in contactless PEC etching [22].

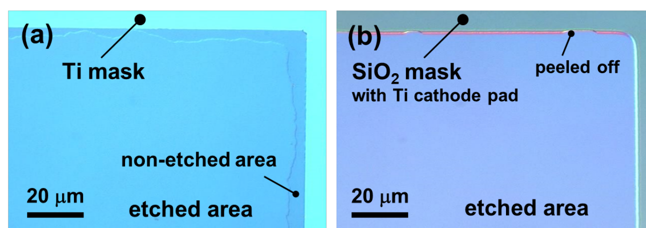

Fig. 10. Typical optical micrographs of contactless PEC-etched AlGaN/GaN HEMT on a SiC substrate. (a) 23.1 nm etched with a Ti mask, (b) 23.2 nm etched with a SiO_2 mask and a Ti cathode pad. The electrolyte was 0.025 M $K_2S_2O_8$ (aq.).

Figure 11 shows typical atomic-force microscopy (AFM) images of the contactless PEC-etched AlGaN/GaN HEMT on SiC substrates. Although bumps remained due to the short carrier lifetime at threading dislocations, the contactless-PEC-etched surface was almost smooth. The surface roughness was almost the same before and after the contactless PEC etching: the arithmetic mean roughness (R_a) in an area of 1 μm^2 was 0.17 nm before etching and 0.22 nm after etching. We also confirmed that the bumps can be removed by the HCl-H_2O_2 post cleaning process accompanied with removing the Ti mask. Furthermore, in contactless PEC etching, the etched depth showed a self-stopping feature similar to that observed in conventional PEC etching [12,17].

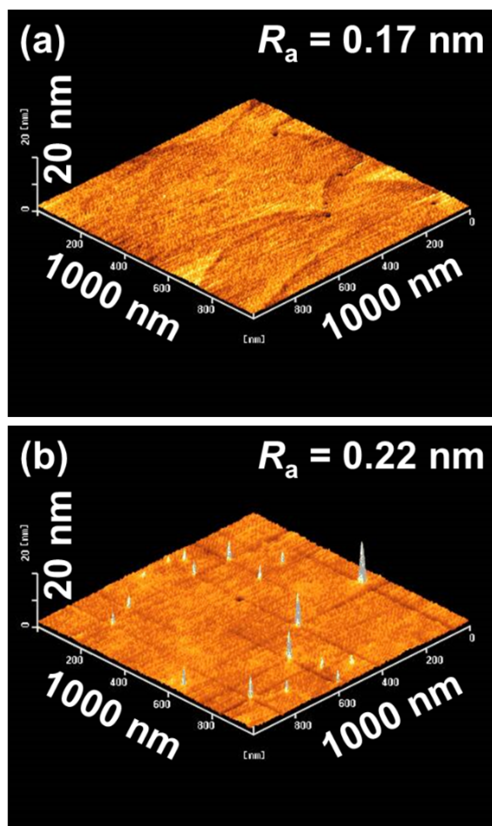

Fig. 11. Typical AFM images of contactless PEC-etched AlGaN/GaN HEMT on SiC substrates. (a) The As-grown surface, (b) 23.1 nm etched with a Ti mask.

The dependence of the offset between the SiO_2 mask and the Ti cathode pad in terms of the fineness of the etched patterns, and the lifetime of the electrolyte remains unclear. Although Maher et al. succeeded in 100-nm isolation etching of an $Al_{0.25}Ga_{0.75}N$[17.5nm]/GaN HEMT by contactless PEC etching with a catalytic Pt mask [26], our results showed a self-stopping feature in an AlGaN barrier layer with a SiO_2 mask with a Ti cathode or Ti mask. Thus, the selectivity of the recess/isolation condition is an ongoing issue in these simple contactless PEC etching technologies.

IV. Conclusions

We successfully fabricated deep trench structures in GaN by PEC etching with a Ti mask. The aspect ratio of these trenches was more than 7 at an etching depth in excess of 20 μm. These results show that PEC etching can be applied to the fabrication of deep trench structures in GaN for the manufacture of SJ devices. In addition, we demonstrated a simple contactless PEC etching of an n-GaN epi layer grown on an n-GaN substrate. TMAH posttreatment was effective in producing vertical side walls. Furthermore, we have discussed the design of cathodes for applying simple contactless PEC etching in the fabrication of RF devices consisting of AlGaN/GaN HEMT on a semi-insulating substrate. Fortunately, AlGaN/GaN HEMT has an ohmic electrode that can act as the cathode in contactless PEC etching; consequently, we succeeded in recess etching of an AlGaN/GaN HEMT epilayer grown on a semi-insulating SiC substrate by using the etching mask with the cathode pad. These results indicate that PEC etching is a feasible process for the fabrication of practical devices.

Acknowledgment

The authors would like to thank the Japan Ministry of the Environment for their support of the project 'Technical Innovation to Create a Future Ideal Society and Lifestyle'. A part of this study was supported by JSPS KAKENHI – JP16H06421, JP17H03224.

References

[1] W. Saito, I. Omura, T. Ogura, and H. Ohashi. (2004, Sep.). Theoretical limit estimation of lateral wide band-gap conductor power-switching device. *Solid-State Electron*. [Online] *48(9)*, pp. 1555–1562. Available: https://doi.org/10.1016/j.sse.2003.10.003

[2] M. Kodama, M. Sugimoto, E. Hayashi, N. Soejima, O. Ishiguro, M. Kanechika, K. Itoh, H. Ueda, T. Uesugi, and T. Kachi. (2008, Feb.). GaN-based trench gate metal oxide conductor field-effect transistor fabricated with novel wet etching. *Appl. Phys. Express* [Online] *1(2)*, pp. 021104-1-3. Available: https://doi.org/10.1143/APEX.1.021104

[3] T. Oka. (2019, Apr.). Recent development of vertical GaN power devices. *Jpn. J. Appl. Phys.* [Online] *58(SB)*, pp. SB0805-1-12. Available: https://doi.org/10.7567/1347-4065/ab02e7

[4] I. Ben-Yaacov, Y.-K. Seck, U. K. Mishra, and S. P. DenBaars. (2004, Jan.). AlGaN/GaN current aperture vertical electron transistors with regrown channels. *J. Appl. Phys.* [Online] *95(4)*, pp. 2073–2078. Available: https://doi.org/10.1063/1.1641520

[5] D. Shibata, R. Kajitani, M. Ogawa, K. Tanaka, S. Tamura, T. Hatsuda, M. Ishida, and T. Ueda. (2016). 1.7 kV/1.0 mΩcm^2 normally-off vertical GaN transistor on GaN substrate with regrown p-GaN/AlGaN/GaN polar

gate structure. Presented at the IEEE International Electron Devices Meeting (IEDM), San Francisco, CA, 2016. [Online] pp. 10.1.1–10.1.4 Available: https://doi.org/10.1109/IEDM.2016.7838385.

[6] M. Sun, Y. Zhang, X. Gao, and T. Palacios. (2017, Apr.). High-performance GaN vertical fin power transistors on bulk GaN substrates. *IEEE Electron Device Lett.* [Online] *38(4)*, pp. 509–512. Available: https://doi.org/10.1109/LED.2017.2670925

[7] V. Unni and E. M. S. Narayanan. (2017, Feb.). Breaking the GaN material limits with nanoscale vertical polarisation super junction structures: A simulation analysis. *Jpn. J. Appl. Phys.* [Online] *56(4S)*, pp. 04CG02-1-5. Available: https://doi.org/10.7567/JJAP.56.04CG02

[8] T. Fujihira. (1997, Oct.). Theory of conductor superjunction devices. *Jpn. J. Appl. Phys.* [Online] *36(1)*, pp. 6254–6262. Available: https://doi.org/10.1143/JJAP.36.6254

[9] Y. Onishi and Y. Hashimoto. (2015, Jan.). Numerical analysis of specific on-resistance for trench gate superjunction MOSFETs. *Jpn. J. Appl. Phys.* [Online] *54(2)*, pp. 024101-1-7. Available: http://dx.doi.org/10.7567/JJAP.54.024101

[10] R. J. Shul, G. B. McClellan, S. A. Casalnuovo, D. J. Rieger, S. J. Pearton, C. Constantine, C. Barratt, R. F. Karlicek, C. Tran, and M. Schurman. (1996, Jun.). Inductively coupled plasma etching of GaN. *Appl. Phys. Lett.* [Online] *69(8)*, pp. 1119–1121. Available: https://doi.org/10.1063/1.117077

[11] N. Medelci, A. Tempez, D. Starikov, N. Badi, I. Berishev, and A. Bensaoula. (2000, Sep.). Etch characteristics of GaN and BN materials in chlorine-based plasmas. *J. Electron. Mater.* [Online] *29(9)*, pp. 1079–1083. Available: https://doi.org/10.1007/s11664-004-0268-6

[12] Y. Kumazaki, K. Uemura, T. Sato, and T. Hashizume. (2017, May). Precise thickness control in recess etching of AlGaN/GaN hetero-structure using photocarrier-regulated electrochemical process. *J. Appl. Phys.* [Online] *121*, pp. 184501-1-6. Available: https://doi.org/10.1063/1.4983013

[13] S. G. Lee, S. Mishkat-UI-Masabih, J. T. Leonard, D. F. Feezell, D. A. Cohen, J. S. Speck, S. Nakamura, and S. P. Denbaars. (2017, Dec.). Smooth and selective photo-electrochemical etching of heavily doped GaN:Si using a mode-locked 355nm microchip laser. *Appl. Phys. Express* [Online] *10(1)*, pp. 011001-1-3. Available: https://doi.org/10.7567/APEX.10.011001

[14] F. Horikiri, Y. Narita, and T. Yoshida. (2018, Jul.). Excellent wet etching technique using pulsed anodic oxidation for homoepitaxially grown GaN layer. *Jpn. J. Appl. Phys.* [Online] *57(8)*, pp. 086502-1-7. Available: https://doi.org/10.7567/JJAP.57.086502

[15] F. Horikiri, H. Ohta, N. Asai, Y. Narita, T. Yoshida, and T. Mishima. (2018, Aug.). Excellent potential of photo-electrochemical etching for fabricating high-aspect-ratio deep trenches in gallium nitride. *Appl. Phys. Express* [Online] *11(9)*, pp. 091001-1-4. Available: https://doi.org/10.7567/APEX.11.091001

[16] N. Asai, H. Ohta, F. Horikiri, Y. Narita, T. Yoshida, and T. Mishima. (2019, Apr.). Impact of damage-free wet etching process on fabrication of high breakdown voltage GaN p–n junction diodes. *Jpn. J. Appl. Phys.* [Online] *58(SC)*, pp. SCCD05-1-4. Available: https://doi.org/10.7567/1347-4065/ab0401

[17] K. Uemura, M. Deki, Y. Honda, H. Amano and T. Sato. (2019, May). Effect of photoelectrochemical etching and post-metallization annealing on gate controllability of AlGaN/GaN high electron mobility transistors. *Jpn. J. Appl. Phys.* [Online] *58(SC)*, pp. SCCD20-1-6. Available: https://doi.org/10.7567/1347-4065/ab06b9

[18] C. Youtsey, I. Adesida, and G. Bulman. (1997, Oct.). Highly anisotropic photoenhanced wet etching of n-type GaN. *Appl. Phys. Lett.* [Online] *71(15)*, pp. 2151–2153. Available: http://dx.doi.org/10.1063/1.119365

[19] J. A. Bardwell, J. B. Webb, H. Tang, J. Fraser, and S. Moisa. (2001, Mar.). Ultraviolet photoenhanced wet etching of GaN in $K_2S_2O_8$ solution. *J. Appl. Phys.* [Online] *89(7)*, pp. 4142–4149. Available: https://doi.org/10.1063/1.1352684

[20] D. H. Van Dorp, J. L. Weyher, M. R. Kooijman, and J. J. Kelly. (2009, Jul.). Photoetching mechanisms of GaN in alkaline $S_2O_8^{2-}$ solution. *J. Electrochem. Soc.* [Online] *156(10)*, pp. D371–D376. Available: https://doi.org/10.1149/1.3183807

[21] F. Horikiri, N. Fukuhara, H. Ohta, N. Asai, Y. Narita, T. Yoshida, T. Mishima, M. Toguchi, K. Miwa, and T. Sato. (2019, Feb.). Simple wet-etching technology for GaN using an electrodeless photo-assisted electrochemical reaction with a luminous array film as the UV source. *Appl. Phys. Express* [Online] *12(3)*, pp. 031003-1-6. Available: https://doi.org/10.7567/1882-0786/ab043c

[22] M. Toguchi, K. Miwa, F. Horikiri, N. Fukuhara, Y. Narita, T. Yoshida, and T. Sato. (2019, May). Electrodeless photo-assisted electrochemical etching of GaN using a H_3PO_4-based solution containing $S_2O_8^{2-}$ ions. *Appl. Phys. Express* [Online] *12(6)*, pp. 066504-1-4. Available: https://doi.org/10.7567/1882-0786/ab21a1

[23] R. Kosugi, S. Ji, K. Mochizuki, H. Kouketsu, Y. Kawada, H. Fujisawa, K. Kojima, Y. Yonezawa, and H. Okumura. (2017, Feb.). Strong impact of slight trench direction misalignment from $[11\bar{2}0]$ on deep trench filling epitaxy for SiC super-junction devices. *Jpn. J. Appl. Phys.* [Online] *56(4S)*, pp. 04CR05-1-4. Available: https://doi.org/10.7567/JJAP.56.04CR05

[24] K. M. Dowling, E. H. Ransom, and D. G. Senesky. (2017, Feb.). Profile evolution of high aspect ratio silicon carbide trenches by inductive coupled plasma etching. *J. Microelectromech. Syst.* [Online] *26(1)*, pp. 135–142. Available: https://doi.org/10.1109/JMEMS.2016.2621131

[25] S. Ji, K. Kojima, R. Kosugi, S. Saito, Y. Sakuma, Y. Tanaka, S. Yoshida, H. Himi, and H. Okumura. (2015, Jun.). Filling 4H-SiC trench towards selective epitaxial growth by adding HCl to CVD process. *Appl. Phys. Express* [Online] *8(6)*, pp. 065502-1-4. Available: http://dx.doi.org/10.7567/APEX.8.065502

[26] H. Maher, D. W. DiSanto, G. Soerensen, C. R. Bolognesi, H. Tang, and J. B. Webb. (2000, Dec.). Smooth wet etching by ultraviolet-assisted photoetching and its application to the fabrication of AlGaN/GaN heterostructure field-effect transistors. *Appl. Phys. Lett.* [Online] *77(23)*, pp. 3833–3835. Available: https://doi.org/10.1063/1.1330226